LA-DC - 8781

INDC 227

INDC (US)-6U

PREPRINT FROM

LOS ALAMOS SCIENTIFIC LABORATORY of the University of California

LOS ALAMOS • NEW MEXICO

THE ^{1}H(n, n) CROSS SECTION AS A NUCLEAR STANDARD

By

John C. Hopkins

PANEL OF I. A. E. A.
ON NUCLEAR STANDARDS NEEDED FOR NEUTRON
CROSS SECTION MEASUREMENTS
(Brussels, 8-12 May 1967)

UNITED STATES
ATOMIC ENERGY COMMISSION
CONTRACT W-7405-ENG. 36

ABSTRACT

The suitability of the $^{1}H(n,n)$ cross section as a primary standard for neutron flux measurements in the energy range above 100 keV is examined. The use of the $^{1}H(n,n)$ cross section in relative measurements, in proton recoil devices, and in counter calibration applications is discussed. The total cross section is well known but the differential elastic cross section is very poorly known. A prescription is given for the calculation of the differential cross section at all energies. The conclusion is that the $^{1}H(n,n)$ cross section would be a suitable primary standard for energies above 100 keV. A recommendation is made for action in three areas: 1) The techniques for flux measurement should be improved; 2) an accurate differential cross section measurement should be made; and 3) a serious theoretical study should be made to calculate the differential and total cross sections from known phase shifts.

1. INTRODUCTION

It has been proposed that the $^1H(n,n)$ cross section, at energies above 100 keV, be used as a primary standard for neutron flux measurement (1). The purpose of this report is to examine that proposal in some detail. First, however, I will define what I mean by standard and then outline the scope of this report.

By cross-section standard I mean a nuclear cross section, accepted as being correct within small but well-defined limits and serving as an accepted value for comparison or as a basis for measurement. The $^1H(n,n)$ cross section will be examined within this framework. The use of this cross section as a standard is discussed in Section 2. Section 3 examines pertinent data along with some semiempirical fits. Section 4 contains a prescription for obtaining the differential cross sections from theoretical work on the nucleon-nucleon interaction and other $^1H(n,n)$ and $^1H(p,p)$ data. Finally, Section 5 gives a brief overall review and a three-point recommendation for future investigations.

We shall see that although more work is desirable in all phases of the $^1H(n,n)$ cross-section program, the most serious stumbling block is our inability to measure a neutron flux accurately with the cross-section data that are available.

2. USE OF THE $^1H(n,n)$ CROSS SECTION AS A STANDARD

There are several criteria for judging the relative merits of various possible standards; The cross section should be accurately known; it should have a reasonably smooth variation with energy; it should have some theoretical basis for interpolation and extrapolation to regions where accurate measurements are lacking; and, finally, the cross section should be large compared to competing reactions.

Other characteristics that should be considered are: The material should be easy to obtain and prepare; it should be easy to assay both chemically and isotopically; and, it should be chemically stable (for example, it should not be affected by air, water, or vacuum).

One or several simple standard detectors should be available. For flux measurements the recoil proton may be detected in a gas proportional counter, telescope, or a polyethylene radiator semiconductor counter (2,3,4,5). For these measurements, standard detectors with well-known efficiencies and corrections would be desirable.

How accurate do the standard cross sections need to be? There are two answers to this question. From the experimentalist's standpoint they need not be much better, say a factor of 4, than his tools with which to use them. For example, if his standard cross sections are known to 0.5 percent but he cannot measure a cross section more accurately than 2 percent then he should devote his energy to improving his flux measuring technique. On the other hand, if we take the viewpoint of the reactor designer who may require, for example, a fission cross section to 0.5 percent, we immediately see that the standard should be 2 to 5 times better, or .1 to .3 percent.

Spaepen has reviewed the accuracy needed from the reactor designer's viewpoint (1). The most stringent accuracies pertain to the fission cross sections. Apparently 0.5 percent accuracy is requested whereas 2 percent would be welcome. Using these figures, Spaepen arrives at a standards accuracy of 0.1 to 0.3 percent for the requested accuracy and 0.4 to 1 percent for the acceptable accuracy.

2.1 $^1H(n,n)^1H$ as a Standard Cross Section for Relative Measurements

Neutron cross sections, measured with time-of-flight techniques, have usually been made relative to some well-known scattering cross section (6,7,8). Above 2 MeV the $^1H(n,n)$ cross section is the most satisfactory. This is not a flux measurement *per se*; however the $^1H(n,n)$ cross section does play the role of a standard. In these cases the accuracy of the measured cross section can be no better than the uncertainty in the differential $^1H(n,n)$ cross section.

2.2 Proton Recoil Methods

2.2.1 Proton Recoil Telescope

Proton recoil telescopes have been used for making accurate neutron flux measurements. Complete descriptions and other references can be found in the papers by Bame *et al*. (4), Perry (3), Johnson (2), and White (5). A telescope consists of a hydrogenous radiator and one or more counters which detect protons recoiling within a well-defined solid angle.

Above a few MeV the main problem associated with the $^1H(n,n)$ cross section in a telescope measurement is the anisotropy. This feature is discussed at length in Sections 3 and 4. Briefly, however, the total cross section is well known whereas the differential cross section is very poorly known. The cross section has been assumed to be isotropic below 10 MeV and symmetric about 90°(c.m.) above 10 MeV, with a form following a very simple relationship. These are not good assumptions when one is aiming for the accuracies that are necessary for a nuclear standard. Note that telescope measurements, which involve 180° scattering, see the maximum anisotropy.

Table I gives the sources of error in the telescope measurement of neutron flux (4). Look first at the 1 to 3 MeV region. The total standard deviation, to two significant figures, is 2.8 percent. If there were no uncertainty in the n-p cross section or anisotropy then the error would be reduced to 2.7 percent. In the 3-10 MeV region the total uncertainty is 2.4 percent and without any uncertainties in the anisotropy or $^{1}H(n,n)$ cross section the resulting error would be 2.1 percent. Above 10 MeV the uncertainty in the anisotropy dominates the total uncertainty and a substantial overall improvement would be obtained with a precisely known differential cross section.

2.2.2 Other Proton Recoil Counters

White has recently obtained very high precision using hydrogen and methane gas proportional counters and a polyethylene radiator semiconductor counter as neutron flux measuring instruments (5). One advantage of these devices over the telescope is that they are less sensitive to the anisotropy of the recoil proton distribution. Table II shows the estimated errors for the hydrogen gas recoil counter as used by White. Obviously an improvement in the $^{1}H(n,n)$ cross section without a simultaneous improvement in all of the remaining factors will not substantially increase the accuracy of a flux measurement.

The accuracy of these various flux measuring devices can only be checked by an intercomparison of one device against another. Bame et al. (4) have reported a comparison between the proton recoil telescope and the associated particle technique for a flux measurement of 14 MeV neutrons from the $T(d,n)^{4}He$ reaction. The standard deviation for each measurement was believed to be ±3 percent. The telescope measurement of the flux was 4 percent higher than that given by the alpha monitor.

White (5) has recently reported an intercomparison of his three detectors and a comparison of one of these with the associated alpha particle technique and one with a calibrated long counter. Table III gives these intercomparisons. These results should be considered extraordinarily good, and are the result of meticulous attention to detail. The conclusion is that with great care one can measure fluxes, with the proton recoil technique, to 2 or 2.5 percent.

It should be pointed out here that these techniques become impractical below about 100 keV because of the difficulty in detecting the recoil protons. This is the reason for suggesting that the $^{1}H(n,n)$ reaction be used as a standard only above 100 keV.

2.2.3 Plastic and Liquid Scintillators

Fast neutron time-of-flight experiments usually employ a plastic or liquid scintillator as a detector (7). The efficiency of this detector, and its associated electronics, must be determined as a function of neutron energy. If a cross section is measured relative to some known cross section, only the relative efficiency need be established. This efficiency can be calculated or measured (17,18). In any case it is almost always related to the $^{1}H(n,n)$ cross section. Plastic and liquid scintillators consist of a mixture of hydrogen and carbon atoms in the ratio of about 1.2 to 1. The effect of the carbon must be included to make the most accurate calculation of the efficiency. This requires a knowledge of the cross sections at all energies up to and including the incident neutron energy. The $^{1}H(n,n)$ cross section is known with sufficient accuracy to satisfy this need, at least up to 20 MeV. The carbon cross sections, however, may be regarded as unknown above 5 MeV. Any effect of anisotropy of the $^{1}H(n,n)$ cross section would be totally negligible, at least up to 20 MeV.

If we neglect the carbon contribution the efficiency for a thin scintillator, is given by

$$E(E) = nh\sigma\left(1 - \frac{B}{E}\right) \tag{1}$$

where n is the number of hydrogen atoms per cm^3 of scintillator,

h is the thickness of the scintillator,

σ is the total $^1H(n,n)$ cross section,

B is the counter bias in MeV, and

E is the neutron energy in MeV.

This formula is approximately correct up to 4 or 5 MeV.

The efficiency calculations are not good enough to rely on without some confirmation from experiment. The most accurate technique for determining the relative efficiency of a detector is to measure the $^1H(n,n)$ differential scattering cross section.

In the laboratory system, the differential cross section is

$$\sigma(\psi) = \frac{1}{\pi}\,\sigma_T \cos\psi \quad . \tag{2}$$

The energy of the scattered neutron is

$$E_n(\text{Lab}) = E_I \cos^2\psi \quad , \tag{3}$$

where E_I is the incident neutron energy.

This method is good at low energies, where the $^1H(n,n)$ cross section is isotropic. Any uncertainty in the anisotropy reflects itself as an uncertainty in the efficiency and subsequently in the cross section to be measured.

Other techniques for measuring efficiency involve measuring the angular distribution or spectrum of various source reactions (19,20). Unfortunately, however, none are known with an accuracy of only a few percent.

3. DATA AND EMPIRICAL FITS

Cross-section requirements for reactor work do not normally extend above 15 MeV. For the evaluation of data, however, it will be instructive to examine the cross sections, particularly the differential cross sections, at considerably higher energies.

3.1 Compilations and Evaluations

The Computer Index of Neutron Data (CINDA) contains a fairly complete compilation of all of the neutron cross-section references (9). Horsley, at Aldermaston, has recently published (10) an evaluation in the energy range up to 20 MeV. Schmidt, at Karlsruhe, has prepared an extensive evaluation (11) which includes the $^{1}H(n,n)$ cross section up to 10 MeV. The Sigma Center, at the Brookhaven National Laboratory, has two compilations of $^{1}H(n,n)$ cross-section data (12,13). Hess, at Livermore, has compiled the pre 1958 $^{1}H(n,n)$ scattering data (14,15) above 10 MeV. Gammel has published a thorough review (16) of the theoretical aspects of the $^{1}H(n,n)$ total and differential cross sections up to 40 MeV, though it is not a compilation or evaluation as such.

3.2 Cross Sections

The $^{1}H(n,n)$ cross section is relatively simple and well understood, not in fine detail perhaps, but in its gross features. This is a very important consideration when choosing a nuclear standard.

The total cross section is equal to the elastic cross section plus the capture cross section. We will see that the capture cross section is insignificant and our concern will be with elastic scattering. We will examine these separately.

3.2.1 Total Cross Section

Gammel (16) has found an analytical form based upon a fit to the data, using the effective range theory. The fit is

$$\sigma_n(E) = 3\pi\,[1.206E + (-1.86 + 0.09415E + 0.0001306E^2)^2]^{-1} + \pi\,[1.206E + (0.4223 + 0.13E)^2]^{-1} \quad (4)$$

where $\sigma_n(E)$ is the total cross section, and

E is the laboratory energy.

The effective range expansion parameters which were derived from this fit are given in Section 4.

This fit is as good as the data that went into it. As new, more accurate, data become available the parameters should be improved. Table IV shows some new data that were not available when Gammel made his fit. However, a word of caution is in order. The data of Engelke and Lebowitz (21,22) imply a very low singlet effective range. Noyes shows (24) that this is inconsistent with the expected magnitude of charge dependent effects in the two nucleon system. Moreover, the data of Engelke and of Lebowitz came from the same laboratory (Columbia). These considerations indicate the need for other experiments, preferably from several laboratories, in the energy region below 5 MeV.

Table V shows a sample of the uncertainties in the cross sections measured by Engelke (21), due to various experimental factors. Note that there are 12 factors with an average uncertainty of a few hundredths of a percent, contributing independently to yield a total uncertainty of a few tenths of a percent. The main point here is that these are very difficult experiments. Any improvement will require a large expenditure of scientific effort.

3.2.2 Capture Cross Section

The capture cross section varies smoothly between 10^{-5} times the elastic cross section at 100 keV to 5×10^{-5} times the elastic cross sections at 20 MeV. For most purposes this cross section could be neglected. There are cases, of course, where capture is very important. An example would be neutrons that are thermalized, as in a large liquid scintillator tank, and then eventually captured. Here, however, the neutrons are not captured at energies above 100 keV.

Data on the $H(n,\gamma)D$ reaction are sparse. Much better numbers exist for the inverse reaction, $D(\gamma,n)H$, the photodisintegration of the deuteron. The two cross sections are related by the relationship

$$\sigma_{n,\gamma}(E_n) = \frac{3k^2}{2K^2} \sigma_{\gamma,n}(E_\gamma) \tag{5}$$

where k and K are, respectively, the wave numbers of the γ-ray and neutron in the center of mass system. Horsley (10) quotes an expression for the capture cross section which he judges to be good to 2%:

$$\begin{aligned} \sigma_{n,\gamma}(E) &= 0.0528E^{-\frac{1}{2}}(1 + 0.2244E)(1 + 0.0103E)^2 \\ &\quad \times (1 + 7.46E + 0.158E^2)^{-1} + 0.143E^{\frac{1}{2}}(4.46 + E)^{-1} \end{aligned} \tag{6}$$

in mb (10). E is the laboratory energy in MeV.

3.2.2 Differential Elastic Cross Section

The elastic scattering cross section, integrated over angle, is approximately equal to the total cross section. This value is reasonably well determined. In this section we will investigate the shape of the differential cross-section curve.

The usual argument is that we can only have S wave interaction up to 9 or 10 MeV (10,11). Above this energy Horsley recommends using the Gammel expression, based perhaps upon the observation that the 90 MeV data

(25) are symmetric about 90°. The center of mass system will always be used here.

The Gammel expression is

$$\sigma(\theta,E_n) = \frac{\sigma_T}{4\pi}(1 + b\cos^2\theta)(1 + \frac{1}{3}b)^{-1} , \quad (7)$$

where

$$b = 2(E/90)^2$$

and E is the laboratory energy in MeV (16).

Gammel also offered an extreme expression

$$\sigma(\theta,E) = \frac{\sigma_T}{4\pi}(1 - b/2\cos\theta + b/2\cos^2\theta)(1 + \frac{1}{6}b)^{-1} . \quad (8)$$

This looks extreme because the data seem to indicate that

$$\sigma(0^\circ,E) > \sigma(90^\circ,E) .$$

The actual form of these expressions is important. For flux measurements using a telescope the counting rate must be multiplied by the ratio of $\sigma_T(E)/4\pi$ to $\sigma(180^\circ,E)$. If either of the Gammel formulas gives results of even approximate validity below 10 MeV, then the anisotropy must be included down to 3 MeV or less to obtain telescope flux measurements to a few tenths of a percent.

A knowledge of the anisotropy is necessary for relative cross-section measurements (see Section 2.1) and for relative efficiency counter calibrations (see Section 2.2.3).

In either of Gammel's two expressions for the differential cross section, the ratio of $\sigma(180^\circ,E)$ to $\sigma(90^\circ,E)$ is $1 + 2(\frac{E}{90})^2$. Figure 1 shows a plot of $2(\frac{E}{90})^2$ versus E on a log-log scale with most of the available data. Measurements were ignored only if they were subsequently superseded by more accurate data at or near the same energy. The points attributed to the data of Scanlon et al. (26) were computed by me. I assumed smooth curves through their data. No errors were assigned to these ratios.

The agreement between Gammel's empirical ratio and the experimental data is impressive. If we take this as evidence that one or the other of Gammel's expressions is right, then we're left with the question: which one is correct in which energy region. Above 30 MeV the data are consistent with a symmetric differential cross section and are not consistent with the extreme expression.

Figure 2 shows the error that would be made in a telescope flux measurement by assuming that one of the two Gammel expressions was correct but that the data were corrected by the wrong expression. This is a log-log plot of the ratio of the 180° cross sections for the two expressions. The maximum percent uncertainty in the 180° cross section is given by

$$\% = 100\,[1/3(\tfrac{E}{90})^2]\,[1 + 1/3(\tfrac{E}{90})^2]^{-1} \quad . \tag{9}$$

There is not much theoretical justification for this procedure. It is only intended as a measure of the state of the ignorance. It can perhaps give some idea of what has to be studied further. For example, Figure 2 says that regardless of which expression we use for the anisotropy we still have 0.1 percent uncertainty due to this anisotropy at 5 MeV.

Figure 3 shows the data on the differential cross section at 14.1 MeV. Stewart (27) has pointed out that all of these data have been normalized in some fashion to the total cross section, but that none, with the possible exception of Seagrave's (28) integrate to a value close to the correct value of 689±5 mb. The errors shown are those quoted by the authors. Also shown on this figure are the cross sections predicted by the Gammel expression and by the extreme expression. The so-called extreme, however, turns out not to give as large a $\sigma(180^\circ)/\sigma(90^\circ)$ ratio as the 1960 calculation by Nakamura (29). With suitable arbitrary normalization, we could probably favor one prediction over another. The value of any such tinkering is open to question.

Figure 4 shows the differential cross section at 22.5 MeV. The solid curve is the fit to the unpublished preliminary data of Leland et al. (30). The expression for this fit is

$$\sigma(\theta) = A_o + A_1 \cos\theta + A_2 \cos^2\theta \quad ,$$

where $\frac{A_1}{A_o} = -0.069 \pm 0.039$, and

$$\frac{A_2}{A_o} = 0.154 \pm 0.057 \quad .$$

The standard deviations are statistical errors only. The curve in Figure 4 has the normalization constant $A_o = 31.2$. Taken together, these three sets of data are consistent with Gammel's symmetric formula.

In summary, I would like to make two points: 1) None of the differential cross-section data are inconsistent with Gammel's expression for a symmetric distribution, and 2) for 0.1 percent accuracy in a flux measurement we must know something about the anisotropy below 10 MeV.

4. CALCULATION OF ^{1}H(n,n) CROSS SECTIONS FROM NUCLEON-NUCLEON INTERACTION THEORY

This section contains a prescription for the calculations of the ^{1}H(n,n) differential cross sections. The derivations of the formulas can be traced through the references cited.

A phase shift analysis of nucleon-nucleon scattering experiments has yielded the differential cross-section expression (31)

$$\sigma(\theta,E) = \frac{1}{2}\left|M_{11}\right|^2 + \frac{1}{4}\left|M_{00}\right|^2 + \frac{1}{4}\left|M_{ss}\right|^2 + \frac{1}{2}\left|M_{10}\right|^2 + \frac{1}{2}\left|M_{01}\right|^2 + \frac{1}{2}\left|M_{1-1}\right|^2 \tag{10}$$

where the M's are the matrix elements in spin space.* The subscripts 1, 0, -1, s on the matrix elements refer to the three triplet states $S_z = +1, 0, -1$ and to the singlet state, respectively.

The matrix elements for ${}^1H(n,n)$ scattering are given by:

$$M_{ss} = (ik)^{-1}\sum_{\text{all }\ell} P_\ell(\theta)\left(\frac{2\ell+1}{2}\right)\alpha_\ell$$

$$M_{11} = (ik)^{-1}\sum_{\text{all }\ell} P_\ell(\theta)\left\{\left(\frac{\ell+2}{4}\right)\alpha_{\ell,\ell+1} + \left(\frac{2\ell+1}{4}\right)\alpha_{\ell,\ell} + \left(\frac{\ell-1}{4}\right)\alpha_{\ell,\ell-1} - \frac{1}{4}\left[(\ell+1)(\ell+2)\right]^{\frac{1}{2}}\alpha^{\ell+1} - \frac{1}{4}\left[(\ell-1)\ell\right]^{\frac{1}{2}}\alpha^{\ell-1}\right\}$$

$$M_{00} = (ik)^{-1}\sum_{\text{all }\ell} P_\ell(\theta)\left\{\left(\frac{\ell+1}{2}\right)\alpha_{\ell,\ell+1} + \left(\frac{\ell}{2}\right)\alpha_{\ell,\ell-1} + \frac{1}{2}\left[(\ell+1)(\ell+2)\right]^{\frac{1}{2}}\alpha^{\ell+1} + \frac{1}{2}\left[(\ell-1)\ell\right]^{\frac{1}{2}}\alpha^{\ell-1}\right\}$$

$$M_{01} = (ik)^{-1}\sum_{\text{all }\ell} P_\ell^{1}(\theta)\left\{-\frac{\sqrt{2}}{4}\left(\frac{\ell+2}{\ell+1}\right)\alpha_{\ell,\ell+1} + \frac{\sqrt{2}}{4}\left(\frac{2\ell+1}{\ell(\ell+1)}\right)\alpha_{\ell,\ell} + \frac{\sqrt{2}}{4}\left(\frac{\ell-1}{\ell}\right)\alpha_{\ell,\ell-1} + \frac{\sqrt{2}}{4}\left(\frac{\ell+2}{\ell+1}\right)^{\frac{1}{2}}\alpha^{\ell+1} - \frac{\sqrt{2}}{4}\left(\frac{\ell-1}{\ell}\right)^{\frac{1}{2}}\alpha^{\ell-1}\right\}$$

$$M_{10} = (ik)^{-1}\sum_{\text{all }\ell} P_\ell^{1}(\theta)\left\{\left(\frac{\sqrt{2}}{4}\right)\alpha_{\ell,\ell+1} - \left(\frac{\sqrt{2}}{4}\right)\alpha_{\ell,\ell-1} + \frac{\sqrt{2}}{4}\left(\frac{\ell+2}{\ell+1}\right)^{\frac{1}{2}}\alpha^{\ell+1} - \frac{\sqrt{2}}{4}\left(\frac{\ell-1}{\ell}\right)^{\frac{1}{2}}\alpha^{\ell-1}\right\}$$

---

* Stapp et al. have labeled the differential cross section I_0. With this exception the notation here will be that of the authors quoted.

$$M_{1-1} = (ik)^{-1} \sum_{\text{all } \ell} P_\ell^{\,2}(\theta) \left\{ \left(\frac{1}{4(\ell+1)}\right) \alpha_{\ell,\ell+1} - \left(\frac{2\ell+1}{4\ell(\ell+1)}\right) \alpha_{\ell,\ell} + \left(\frac{1}{4\ell}\right) \alpha_{\ell,\ell-1} - \frac{1}{4} [(\ell+1)(\ell+2)]^{-\frac{1}{2}} \alpha^{\ell+1} - \frac{1}{4} [(\ell-1)\ell]^{-\frac{1}{2}} \alpha^{\ell-1} \right\} ,$$

where the matrix elements of α may be expressed

$$\alpha_\ell = e^{2i\delta\ell} - 1 ,$$

$$\alpha_{\ell j} = e^{2i\delta\ell j} - 1 , \qquad \text{for } \ell = j ,$$

and if we restrict ourselves to the nuclear bar phase shifts, then (31)

$$\alpha_{j\pm1,j} = \cos 2\epsilon_j \exp(2i\delta_{j\pm1,j}) - 1 , \text{ and}$$

$$\alpha^j = i \sin 2\epsilon_j \exp[i(\delta_{j+1,j} + \delta_{j-1,j})] .$$

Complete sets of phase shifts have been reported (32). Phase shifts, however, change and are updated frequently, as new experimental data are analyzed. To make the best calculations the most accurate phase shifts should be used.

If we restrict ourselves now to S waves, we see that the elastic scattering is isotropic and the total cross section is just $4\pi\ \sigma(\theta)$ elastic. This is then given by

$$\sigma_T = \frac{3\pi}{k^2} \sin^2\delta_t + \frac{\pi}{k^2} \sin^2\delta_s , \tag{11}$$

where δ_t is the S wave triplet phase shift,

δ_s is the S wave singlet phase shift,

k is the neutron wave number, and

$k^2 = 0.01206\ E_{lab} \times 10^{26}\ \text{cm}^{-2}$.

A useful parametric representation of the S wave $^1H(n,n)$ total cross-section data can be obtained by expansion of the quantity k cot δ as a power series in k^2. The same type of expansion can be made for both triplet and singlet phase shifts. If three terms are retained in the two expansions, the total S wave $^1H(n,n)$ cross section can be written in terms of six parameters (21):

$$\sigma = 3\pi \{k^2 + [1/a_t - (k^2/2)\ r_{ot}(1 - 2P_t r_{ot}{}^2 k^2)]^2\}^{-1} + \pi \{k^2 + [1/a_s - (k^2/2)\ r_{os}(1 - 2P_s r_{os}{}^2 k^2)]^2\}^{-1} \quad . \qquad (12)$$

The six parameters are:

a_t: triplet scattering length

a_s: singlet scattering length

r_{ot}: triplet effective range

r_{os}: singlet effective range

P_t: triplet shape parameter

P_s: singlet shape parameter

The results of many experiments must be combined and evaluated to arrive at a set of parameters. Table VI gives the parameters determined or recommended by several authors (11,16,21,22,33). This table is not complete. It is intended only to give an idea on agreement between the various authors. The most accurate are probably the values of Noyes (33). The first column gives the values that were obtained by Gammel from his fit (Eq. 4) to the experimental values of the total cross sections (16). The second column gives the best values at the time (1958). The two reasons that the values in column one do not agree with the values in column two are: 1) that in working out the fit the contributions to the total cross section of states with L ≥ 1, were ignored, and 2) the fact that the triplet parameters are not independent of each other was ignored. All that was required of the numerical coefficients was that the values of the effective range expansion parameters should be roughly realistic, as they are. The values in the column labeled Schmidt are the "best values" available in 1952. These give a reasonable fit to the total cross section below 10 MeV, but they are obsolete and there is no good reason to retain them.

S wave scattering will always give an isotropic differential cross section. Partial waves with an orbital angular momentum greater than zero must be included to investigate the anisotropy in the cross section. The main problem boils down to selecting the proper phase shifts.

The effective range expansion is useful for calculating the singlet and triplet S wave phase shifts. The mixing parameter, ϵ_1, is calculated using the technique of Wong (34). The triplet P phase shifts can be determined from a recent analysis of the p-p scattering parameters (35). A k^3 dependence of the P wave phase shifts is used to extrapolate these values to low energies. The D wave phase shifts, which are small at low energies, are given at 10 MeV by Hamada and Johnston (32). A k^5 dependence of the D wave phase shifts is invoked to extrapolate these to low energies.

5. SUMMARY AND RECOMMENDATIONS

The $^1H(n,n)$ cross section would be a suitable cross-section standard for neutron flux measurements above 100 keV. Up to 7 or 8 MeV the cross sections are known to an accuracy higher than the flux measuring techniques justify. Above 7 or 8 MeV the telescope measurements could be limited by the uncertainties in the differential cross section. The total cross section (Eq. 4) is known more accurately than 2 percent in the region up to 30 MeV. The differential cross section can be assumed to follow Gammel's semiempirical form

(Eq. 7), at least around 14 MeV, with an uncertainty of half of the anisotropy from 90° to 180° and equal to the anisotropy from 0° to 90°.

There are three lines of attack that I think should be pursued:

1) The techniques for measuring flux should be improved. This is by far the most difficult task.

2) A good differential cross-section measurement should be made between 10 MeV and 20 MeV. The relative accuracy should be at least 1 percent at 10 MeV and 3 percent at 20 MeV. This should not be a telescope measurement. It should cover both forward and backward angles. A measurement at less than 10 MeV would be worthwhile if sufficient accuracy were attainable. This is not likely at the present time.

3) A serious effort to calculate differential and total cross sections from phase shift analysis is needed. Gammel's 1957 semiempirical fit (Eq. 4) could certainly be improved upon in light of the newer data. With no additional data the present total cross sections could be determined better than 1 percent and the anisotropies in the differential cross sections perhaps to 30 percent at all energies.

ACKNOWLEDGMENTS

I would like to thank L. Stewart, J. D. Seagrave, R. B. Perkins, R. K. Smith, L. Heller, and J. E. Simmons for their consultations on various phases of this project.

REFERENCES

(1) J. Spaepen, Conf. on Nuclear Data, Paris, 1966.

(2) C. H. Johnson, Fast Neutron Physics, Part I, p. 247 (Interscience Pub., Inc., New York, 1960).

(3) Joseph E. Perry, Jr., Fast Neutron Physics, Part I, Ch. IVB, p. 623 (Interscience Pub., Inc., New York, 1960).

(4) S. J. Bame, Jr., E. Haddad, J. E. Perry, Jr., and R. K. Smith, Rev. Sci. Instr. 28, 997 (1957); Rev. Sci. Instr. 29, 652 (1958); and Rev. Sci. Instr. 31, 911 (1960).

(5) P. H. White, J. Nucl. Energy A/B 19, 325 (1965).

(6) J. C. Hopkins and M. G. Silbert, Nucl. Sci. and Eng. 19, 431 (1964).

(7) J. H. Towle and W. B. Gilboy, Nucl. Phys. 32, 610 (1962).

(8) L. Cranberg and J. S. Levin, Phys. Rev. 109, 2063 (1958).

(9) Computer Index of Neutron Data (CINDA), EANDC 60 "U", July 1, 1966 and Oct. 15, 1966, Suppl. 1.

(10) A. Horsley, AWRE Report 0-23/65 (July 1965) and Nucl. Data 2, 243 (1966).

(11) J. J. Schmidt, KFK 120, EANDC-E-35 "U", Feb. 1966.

(12) J. R. Stehn, M. D. Goldberg, B. A. Magurno, and R. Wiener-Chasman, BNL 325, 2nd ed., Suppl. 2 (1964).

(13) M. D. Goldberg, V. M. May, and J. R. Stehn, BNL 400, Vol. 1, 2nd ed. (Oct. 1962).

(14) Wilmot N. Hess, UCRL-4639 (Jan. 1956).

(15) Wilmot N. Hess, Rev. Mod. Phys. 30, 368 (1958).

(16) J. L. Gammel, Fast Neutron Physics, Part II, Ch. VI, p. 2185 (Interscience Pub., Inc., New York, 1960).

(17) R. Batchelor, W. B. Gilboy, J. B. Parker, and J. H. Towle, Nucl. Instr. and Methods 13, 70 (1961).

(18) B. V. Rybakov and V. A. Sidorov, Fast-Neutron Spectroscopy, Suppl. 6, Soviet J. of Atomic Energy, 1959 (Consultants Bureau, Inc., New York, 1960).

(19) J. A. Cookson, D. Dandy, and J. C. Hopkins, Nucl. Phys. A91, 273 (1967).

(20) J. B. Czirr, D. R. Nygren, and C. D. Zafiratos, Nucl. Instr. and Methods 31, 226 (1964).

(21) C. E. Engelke, R. E. Benenson, E. Melkonian, and J. M. Lebowitz, Phys. Rev. 129, 324 (1963).

(22) J. Lebowitz, WASH-1048, 21 (1964).

(23) D. E. Groce and B. D. Sowerby, Nucl. Phys. 83, 199 (1966); D. E. Groce, B. D. Sowerby, and J. M. Morris, Phys. Lett. 17, 40 (1965).

(24) H. Pierre Noyes, Nucl. Phys. 74, 508 (1965).

(25) C. Storrs and D. Frisch, Phys. Rev. 95, 1252 (1954).

(26) J. P. Scanlon, G. H. Stafford, J. J. Thresher, and P. H. Bowen, Nucl. Phys. 41, 401 (1963).

(27) Leona Stewart (private communication, April 1967).

(28) J. D. Seagrave, Phys. Rev. 97, 757 (1955).

(29) J. Nakamura, J. Phys. Soc. Japan 15, 1359 (1960).

(30) W. Leland, J. Beery, H. Bryant, and E. Flynn (private communication, 1967).

(31) H. P. Stapp, T. J. Ypsilantis, and N. Metropolis, Phys. Rev. 105, 320 (1957).

(32) T. Hamada and I. D. Johnston, Nucl. Phys. 34, 382 (1962).

(33) H. Pierre Noyes, Phys. Rev. 130, 2025 (1963).

(34) David Y. Wong, Phys. Rev. Letters 2, 406 (1959).

(35) H. Pierre Noyes (private communication from Leon Heller, April 1967).

TABLE I: Sources of error in telescope measurement of neutron flux, for several energies of neutron energy. From Bame et al. (4).

Source of error	Standard Error (percent) 1-3 MeV	3-10 MeV	10-20 MeV	20-30 MeV
Total n-p cross section	0.5	0.5	0.7	1.5
Anisotropy of n-p scattering	0.2	1.0	2.0	3.0
Protons per cm^2 of radiator	0.5	0.5	0.5	0.5
Geometry of counter and source	1.0	1.0	1.0	1.0
Scattering and attenuation of neutrons	1.5	1.0	0.5	0.5
Various backgrounds	2.0	1.5	1.0	2.0
$[\Sigma\ (\text{Standard error})^2]^{\frac{1}{2}}$	2.8	2.4	2.6	4.1

TABLE II: Estimated error in the flux measurement introduced by various factors. Hydrogen gas recoil counter. Neutron energy 150 keV. From White (5).

Source of Uncertainty		Percent Uncertainty
Determination of recoil counter volume		0.2
Determination of recoil counter pressure		0.5
Statistical error on theoretical recoil proton spectrum		0.7
Error in fitting recoil proton spectrum		1.2
Recoil counter scattering corrections		0.4
Distance measurements		1.0
Air attenuation		0.3
$^{1}H(n,n)$ scattering cross section		0.5
	Total	2.1

TABLE III: Intercomparison of neutron flux counters. From White (5).

Counters	Energy (MeV)	Ratio $\frac{\text{Flux from 1st counter}}{\text{Flux from 2nd counter}}$
H_2 gas recoil counter vs. CH_4 gas recoil counter	0.500	0.98 ± 0.02
CH_4 gas recoil counter vs. semiconductor recoil counter	1.0	0.93 ± 0.04
CH_4 gas recoil counter vs. semiconductor recoil counter	2.25	0.975± 0.03
Semiconductor recoil counter vs. recoil telescope	5.0	1.03 ± 0.05
Recoil telescope vs. α-particle yield from the d-T reaction	14.1	0.98 ± 0.03
H_2 gas recoil counter vs. calibrated long counter	0.200	1.01 ± 0.03

TABLE IV: Hydrogen total cross sections part of table from Spaepen (1).

Reference	Energy (MeV)	Measured $\sigma_{n,n}$ barns	Calculated $\sigma_{n,n}$ (Gammel fit)	Discrep. %
Engelke (21)	0.4926	6.202 ± 0.18%	6.209	-0.11
Engelke (21)	3.205	2.206 ± 0.31%	2.187	+0.86
Lebowitz (22)	3.204	2.212 ± 0.17%	2.187	+1.13
Lebowitz (22)	5.858	1.465 ± 0.16%	1.446	+1.3
Groce (23)	19.565	0.493 ± .49%	0.496	- .61
Groce (23)	23.951	0.397 ± .43%	0.400	- .76
Groce (23)	27.950	0.338 ± .62%	0.336	+ .60

TABLE V: Uncertainties in the measured total cross section due to various experimental factors. From Engelke *et al.* (21).

		At 0.4926 MeV (percent)	At 3.205 MeV (percent)
(1)	Counting statistics	±0.095	±0.15
(2)	Neutron energy uncertainty	±0.067	±0.13
(3)	Inscattering correction uncertainty	±0.101	±0.20
(4)	Length of sample uncertainty	±0.05	±0.03
(5)	Heptane average density uncertainty	±0.05	±0.05
(6)	Graphite blank density uncertainty	±0.02	±0.02
(7)	Gamma-ray background uncertainty	±0.02	±0.00
(8)	Neutron background uncertainty	±0.02	±0.03
(9)	Heptane purity uncertainty	±0.01	±0.01
(10)	Rate dependence uncertainty	±0.01	±0.10
(11)	Multiple inscattering uncertainty	±0.005	±0.10
(12)	Uncertainty due to measurement of difference in end wall thickness of same holder and blank holder	±0.02	±0.05
Net uncertainty		±0.18	±0.31

TABLE VI: Various S wave scattering parameters, determined or recommended by various authors.

	Gammel (16) σ_T Fit	Gammel (16) Best Values	Schmidt (11)	Engelke (21) Lebowitz (22)	Noyes (33)
a_t	5.376 f	5.40 f	5.378± .020 f		5.396±0.011 f
a_s	-23.68 f	-23.75 f	-23.69 ± .05 f		-23.678±0.028 f
r_{ot}	1.56 f	1.7562 f	1.7 ±0.03 f		1.726±0.014 f
r_{os}	2.156 f	2.60 f	2.7 ±0.5 f	2.46±0.12	2.51 ±0.11 f
P_t	-0.03	-0.04	0		
P_s	0	-0.02	0		

FIGURE CAPTIONS

Figure 1. In either of Gammel's two expressions for the differential cross section, the ratio of $\sigma(180^\circ,E)$ to $\sigma(90^\circ,E)$ is $1+2(E/90)^2$. This figure shows a plot of $2\left(\frac{E}{90}\right)^2$ versus E on a log-log scale with most of the available data (16).

Figure 2. This figure shows the error that would be made in a telescope flux measurement by assuming that one of the two Gammel expressions was correct but that the data were corrected by the wrong expression. This is a log log plot of the ratio of the 180° cross sections for the two expressions.

Figure 3. The data on the differential cross section at 14.1 MeV.

Figure 4. The data on the differential cross section at 22.5 MeV.

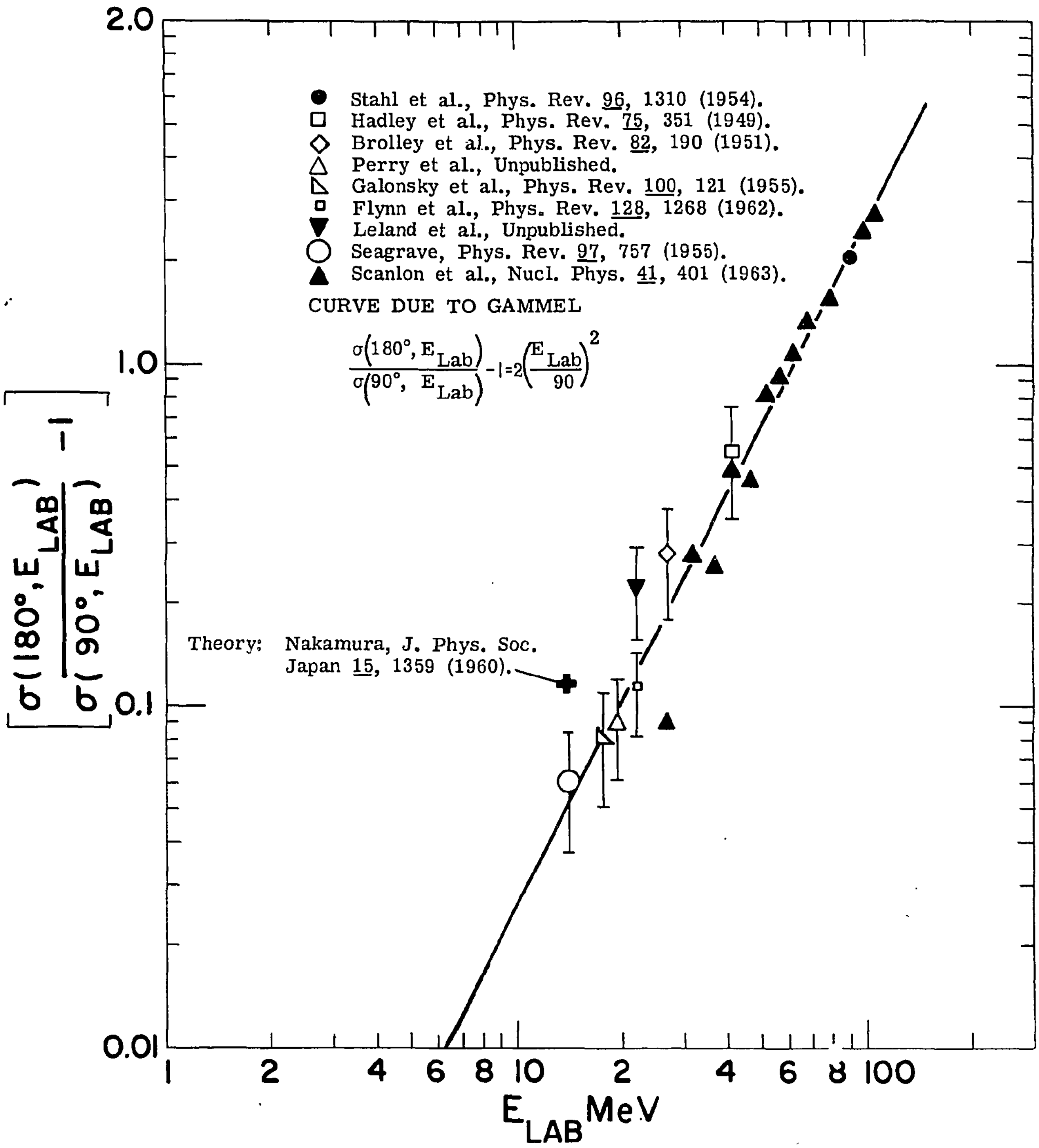
2.0
1.0
0.1
0.01
1 2 4 6 8 10 2 4 6 8 100
E_{LAB} MeV
$\left[\dfrac{\sigma(180°, E_{LAB})}{\sigma(90°, E_{LAB})} - 1\right]$
Stahl et al., Phys. Rev. 96, 1310 (1954).
Hadley et al., Phys. Rev. 75, 351 (1949).
Brolley et al., Phys. Rev. 82, 190 (1951).
Perry et al., Unpublished.
Galonsky et al., Phys. Rev. 100, 121 (1955).
Flynn et al., Phys. Rev. 128, 1268 (1962).
Leland et al., Unpublished.
Seagrave, Phys. Rev. 97, 757 (1955).
Scanlon et al., Nucl. Phys. 41, 401 (1963).
CURVE DUE TO GAMMEL
$\dfrac{\sigma(180°, E_{Lab})}{\sigma(90°, E_{Lab})} - 1 = 2\left(\dfrac{E_{Lab}}{90}\right)^2$
Theory: Nakamura, J. Phys. Soc. Japan 15, 1359 (1960).

Figure 1

MAXIMUM PERCENT UNCERTAINTY
IN σ (180°) FROM ANISOTROPY

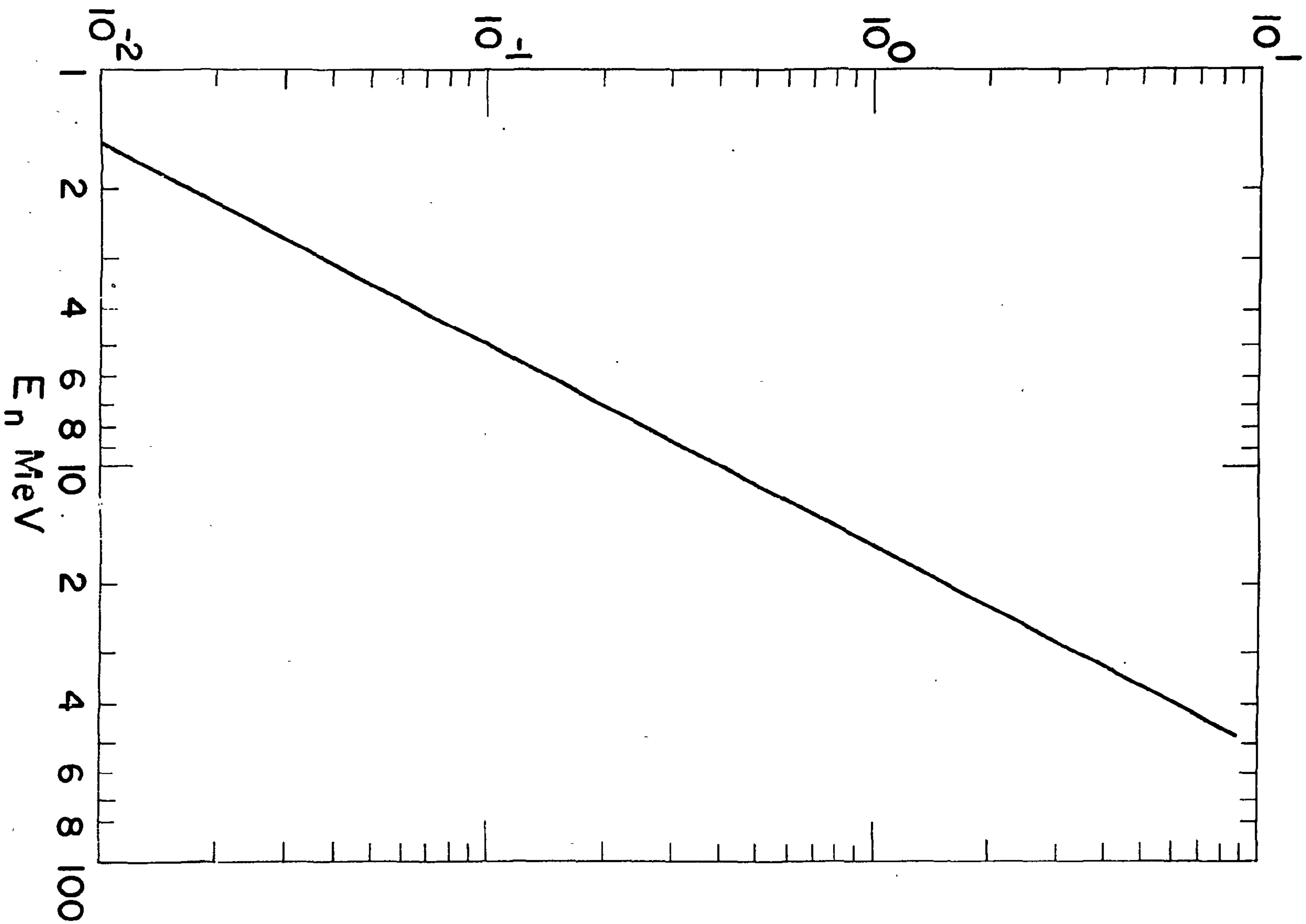

Figure 2

Figure 3

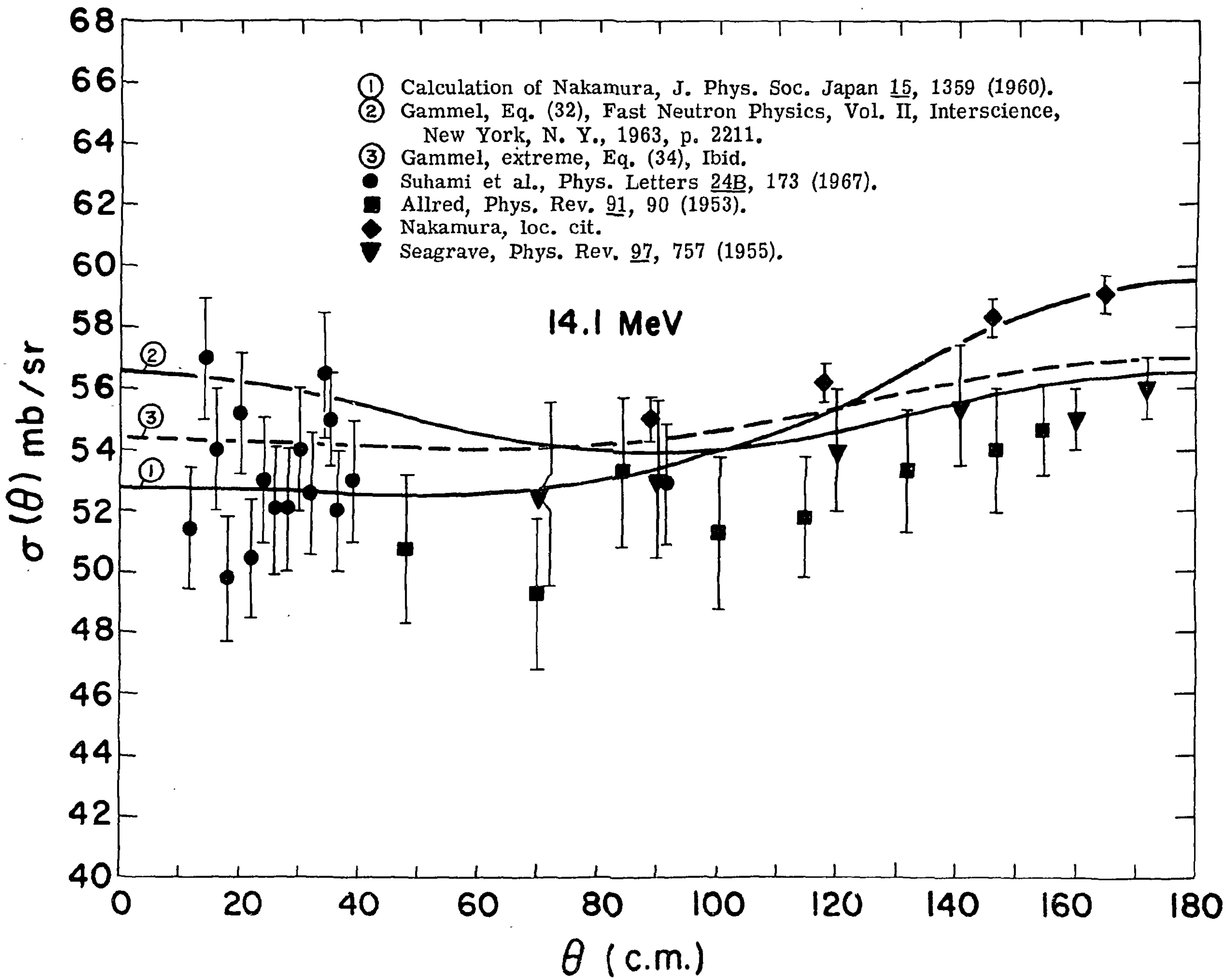

① Calculation of Nakamura, J. Phys. Soc. Japan 15, 1359 (1960).
② Gammel, Eq. (32), Fast Neutron Physics, Vol. II, Interscience, New York, N. Y., 1963, p. 2211.
③ Gammel, extreme, Eq. (34), Ibid.
● Suhami et al., Phys. Letters 24B, 173 (1967).
■ Allred, Phys. Rev. 91, 90 (1953).
◆ Nakamura, loc. cit.
▼ Seagrave, Phys. Rev. 97, 757 (1955).
14.1 MeV
σ (θ) mb/sr
θ (c.m.)
68
66
64
62
60
58
56
54
52
50
48
46
44
42
40
0
20
40
60
80
100
120
140
160
180

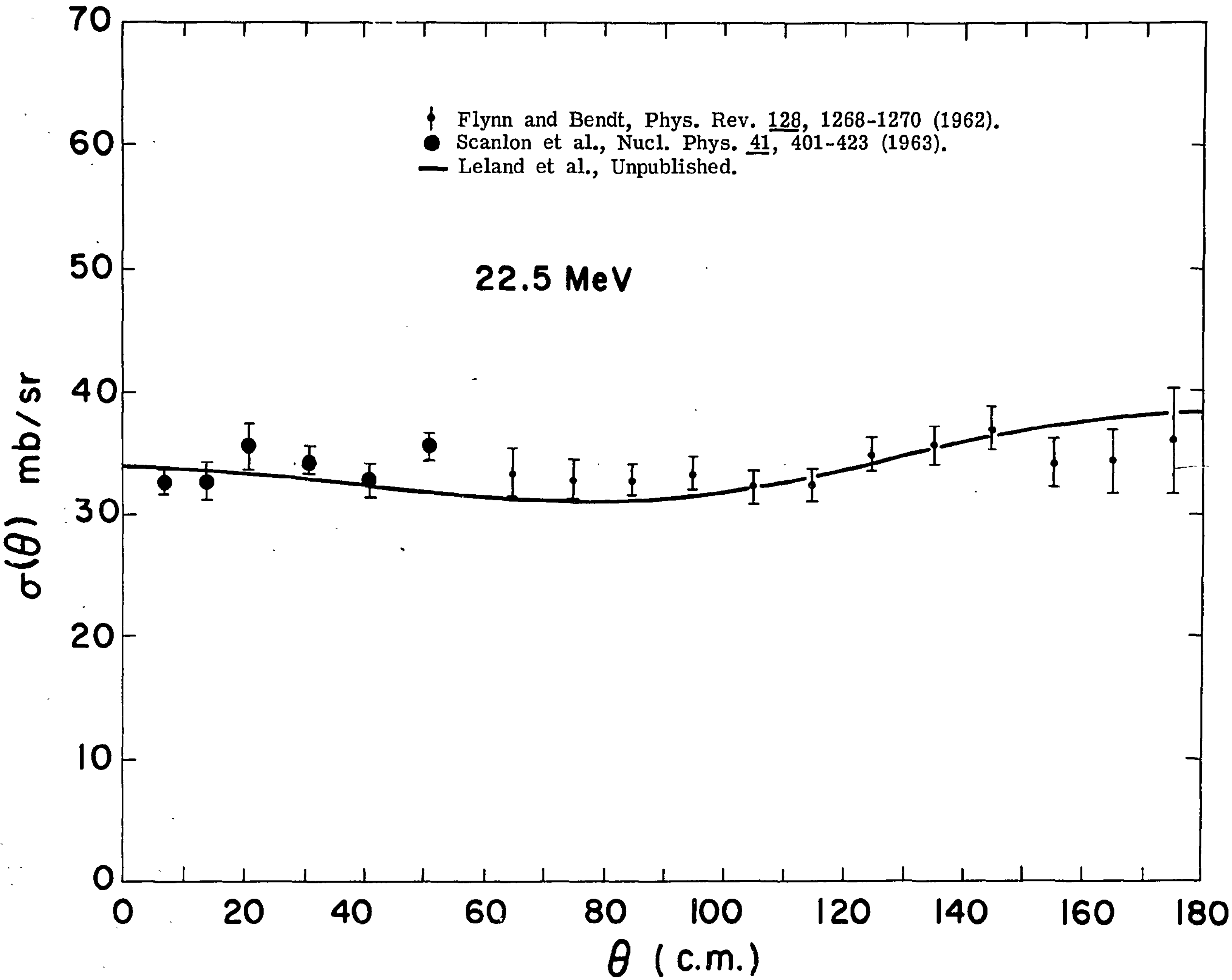
Flynn and Bendt, Phys. Rev. 128, 1268-1270 (1962).
Scanlon et al., Nucl. Phys. 41, 401-423 (1963).
Leland et al., Unpublished.
22.5 MeV
$\sigma(\theta)$ mb/sr
θ (c.m.)
0
10
20
30
40
50
60
70
0
20
40
60
80
100
120
140
160
180

Figure 4